

# Recognition of Platinum-DNA adducts by HMGB1a

*Srinivas Ramachandran<sup>1</sup>, Brenda Temple<sup>2</sup>, Anastassia N. Alexandrova<sup>3</sup>, Stephen G. Chaney<sup>1,\*</sup> and Nikolay V. Dokholyan<sup>1,\*</sup>*

<sup>1</sup>Department of Biochemistry and Biophysics, <sup>2</sup>R. L. Juliano Structural Bioinformatics Core Facility, University of North Carolina at Chapel Hill, <sup>3</sup>Department Chemistry and Biochemistry, University of California at Los Angeles, CA 90095-1569, USA

\*Corresponding Authors: Nikolay V. Dokholyan, 3097 Genetic Medicine Building, Campus Box 7260, Chapel Hill, NC 27599, E-mail: dokh@unc.edu, Phone: 919-843-2513 and Stephen G. Chaney, 3091 Genetic Medicine Building, Campus Box 7260, Chapel Hill, NC 27599, E-mail: sgc@med.unc.edu

## **SUPPORTING INFORMATION**

5' CCTCTC**TGG**ACCTTCC 3'  
3' GGAGAG**ACCT**GGAAGG 5'

5' CCTCTC**AGG**CCTTCC 3'  
3' GGAGAG**TCC**GGAAGG 5'

5' CCTCTC**TGG**TCTTCC 3'  
3' GGAGAG**ACC**AAGG 5'

**Figure S1. DNA sequences used in the Pt-DNA-HMGB1a simulations.** The base-pair step containing the platinated guanines is colored red. The bases flanking the Pt adduct are colored green.

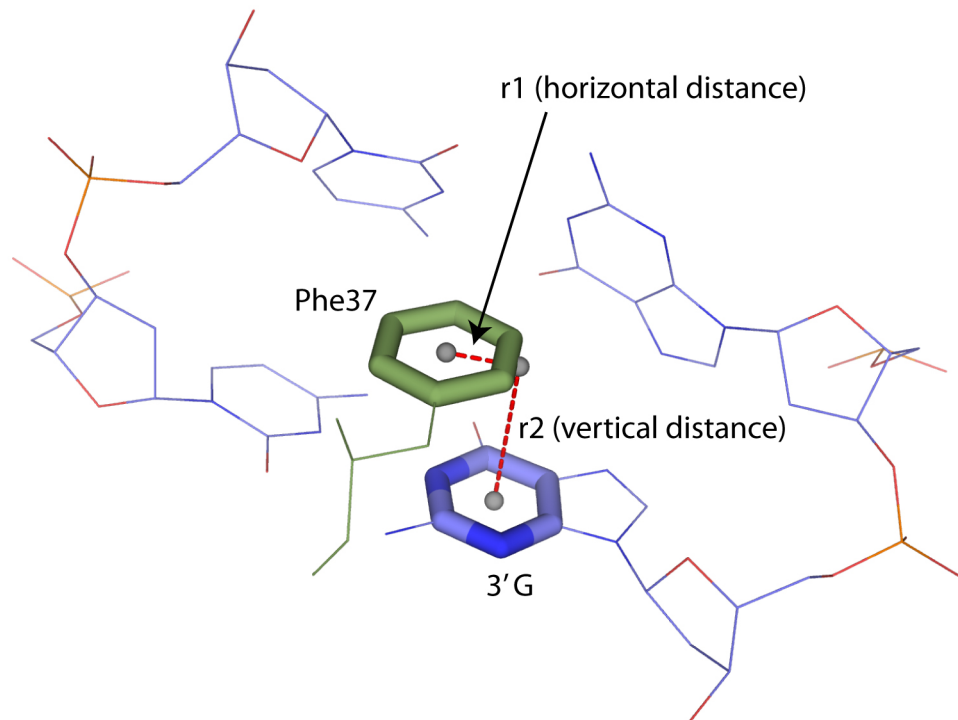


**Figure S2. Geometric characterization of stacking interactions.** The six-membered rings of the stacking residues (Phe37 and 3' G of the Pt-GG base-pair step) are shown as sticks. The grey spheres represent the points of reference to calculate the horizontal and vertical distances.

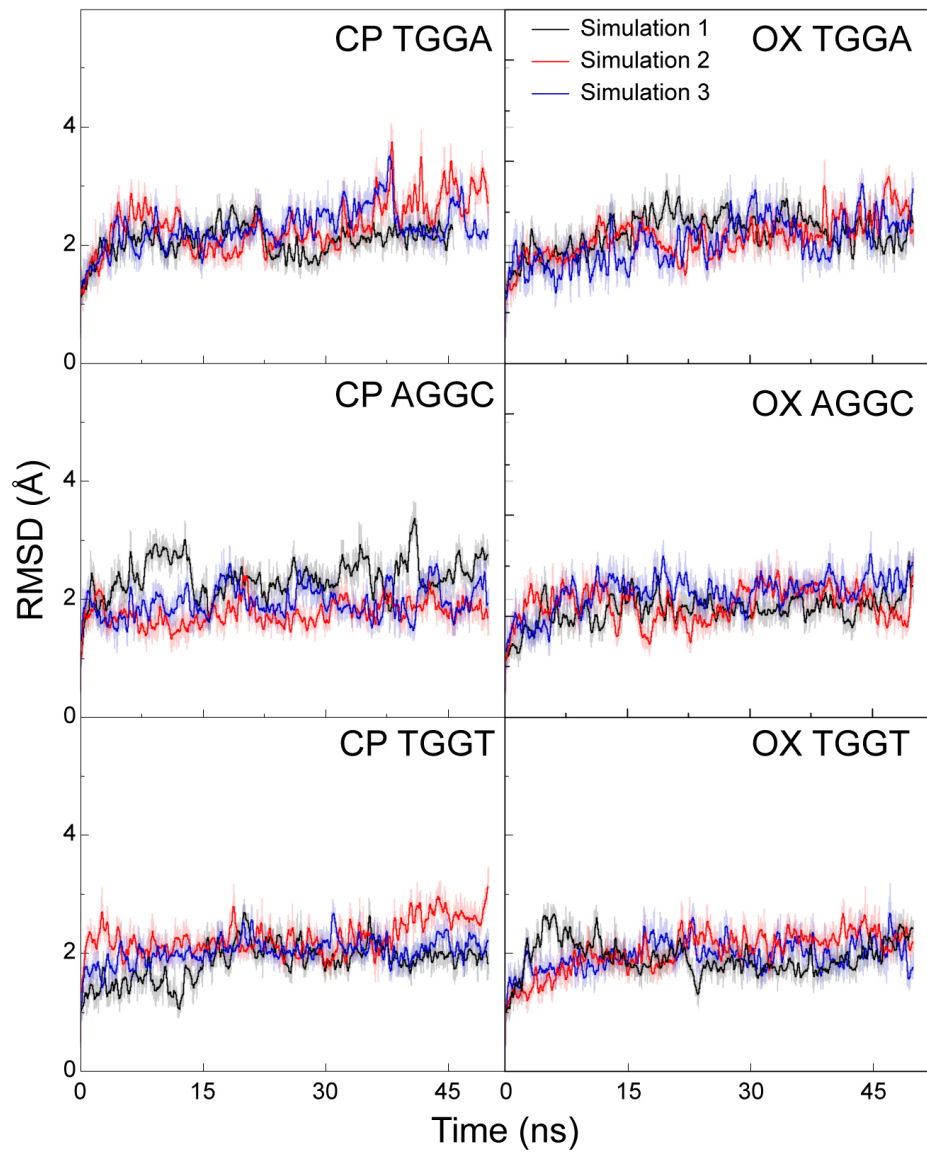


**Figure S3. Average RMSD values for the MD simulations over time.** The RMSD values for each of the 3 simulations are compared to the corresponding starting structure. RMSD at time  $t$  represents the average of RMSD in a 300 ps bin centered at  $t$  (running average).

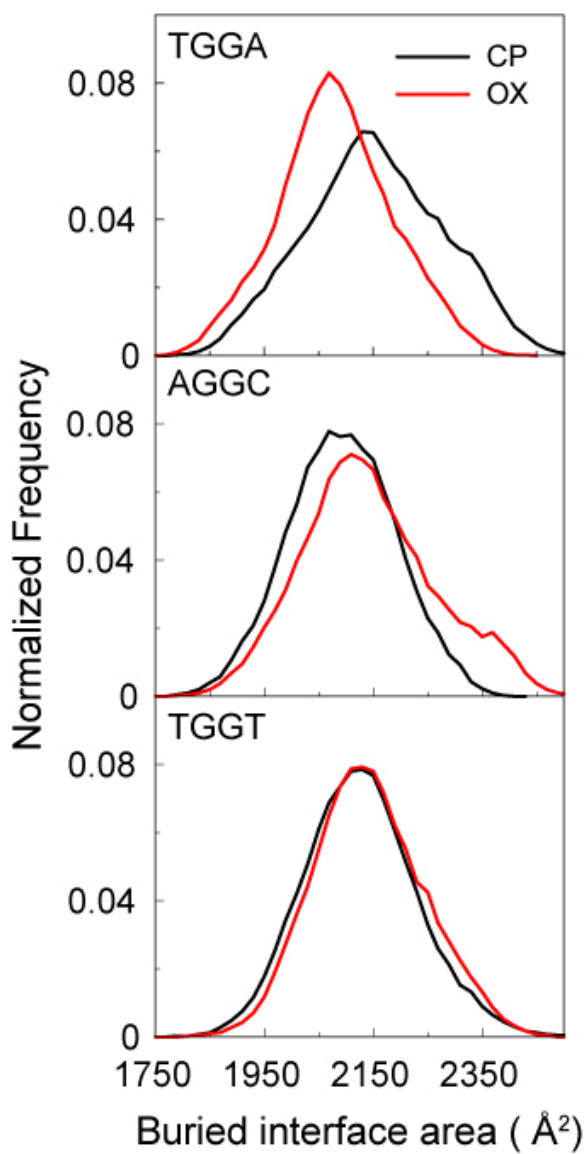


**Figure S4. Distribution of the buried interface area.** The distributions of the solvent accessible surface area that is buried by the formation of the protein-DNA interface are plotted for CP- and OX-DNA in the TGGA, AGGC and TGGT sequence contexts.

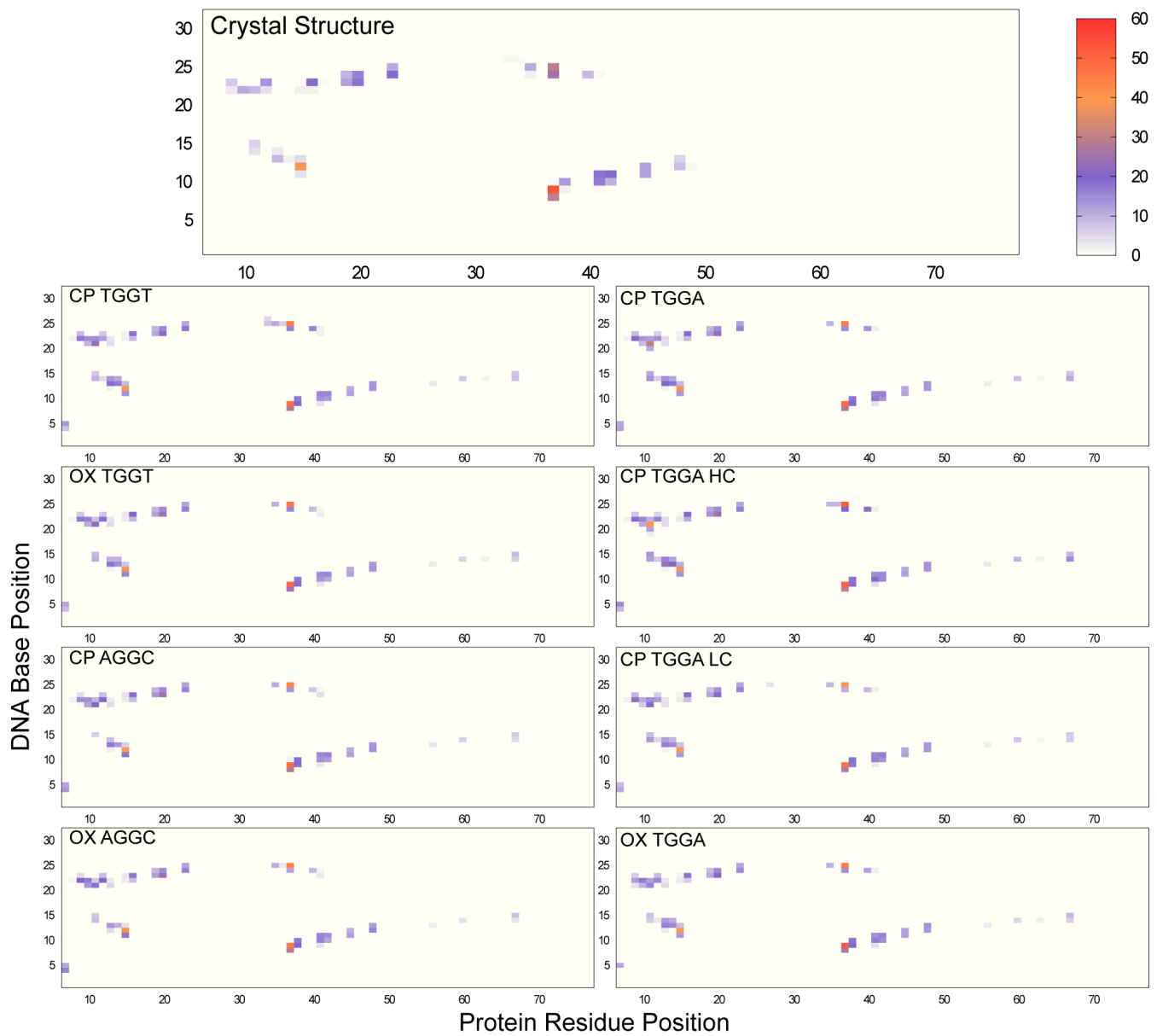


**Figure S5. Pt-DNA-HMGB1a contact map.** Each square on the contact map represents the interaction between a protein residue and a DNA base. The color of the square indicates the average number of heavy atom contacts involving the residue and the base. The scale of color used is shown on right. The contact maps are plotted for the crystal structure (A), the overall OX-DNA ensemble (B), the high contact ensemble (C) and low contact ensemble (D) of CP-DNA.

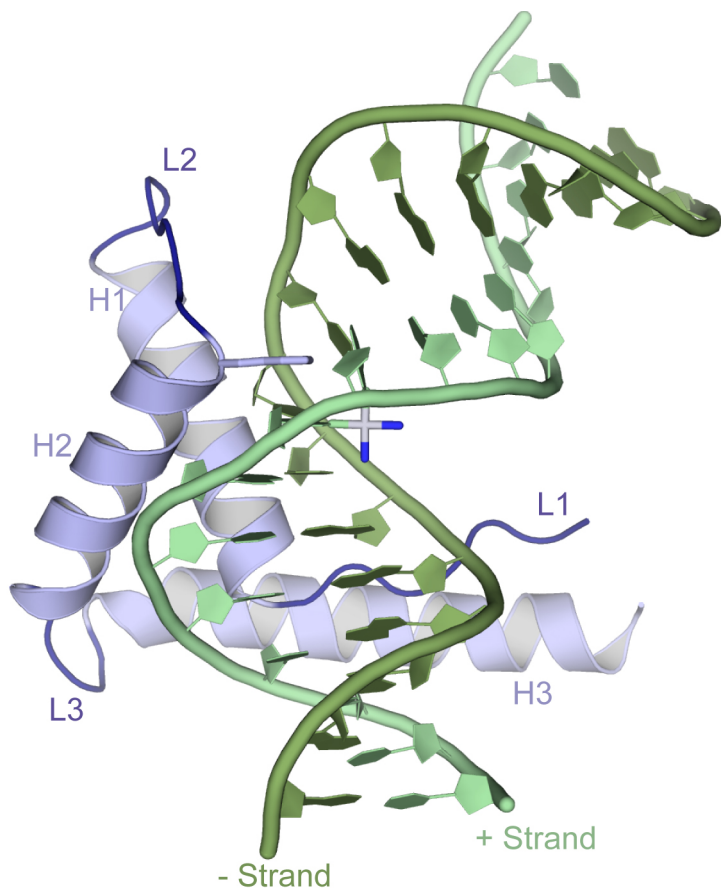


**Figure S6. Crystal structure of CP-TGGA-HMGB1a complex.** The structure is shown using cartoon representation with Phe37 and CP represented as sticks. The different segments of HMGB1a (L1, H1, L2, H2, L3 and H3) are labeled.

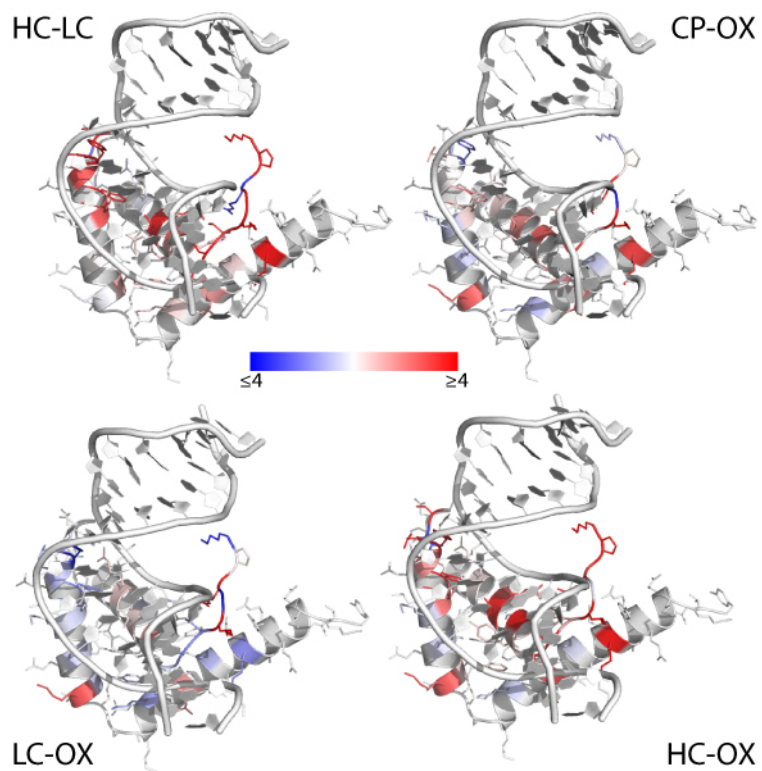


**Figure S7. Differential contact frequency of MD ensembles represented on the Pt-DNA-HMGB1a complex.** The difference contact map of comparing HC-CP-TGGA to LC-CP-TGGA, CP-TGGA to OX-TGGA, LC-CP-TGGA to OX-TGGA and HC-CP-TGGA to OX-TGGA are labeled as HC-LC, CP-OX, LC-OX and HC-OX respectively. Positive differences (indicating increased contacts in the first ensemble compared to second) are colored red and negative differences are colored blue (indicated in the scale at the center).

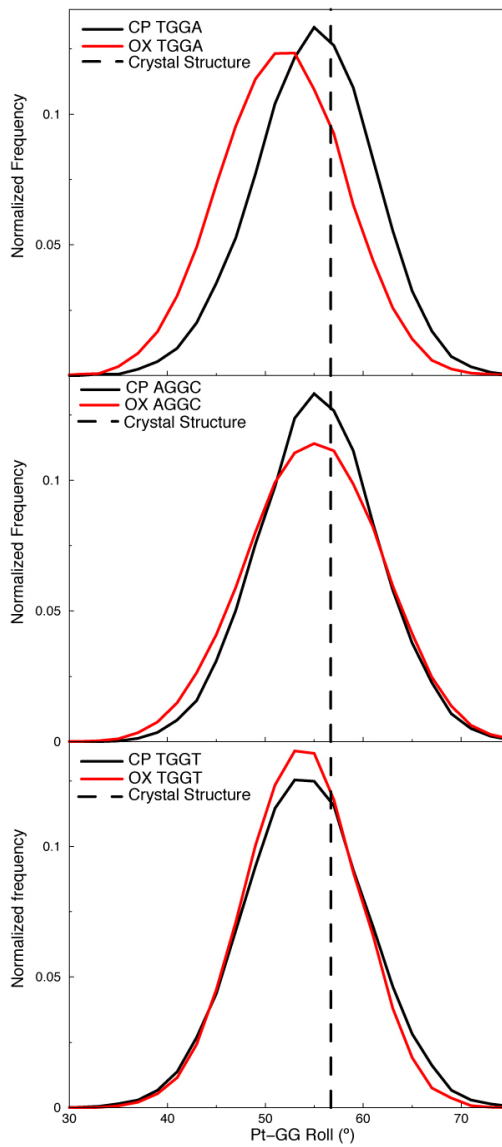


**Figure S8. Roll of Pt-GG base-pair step calculated using CURVES.** The value of the roll in the CP-TGGA-HMGB1a crystal structure is indicated by a dashed vertical line.

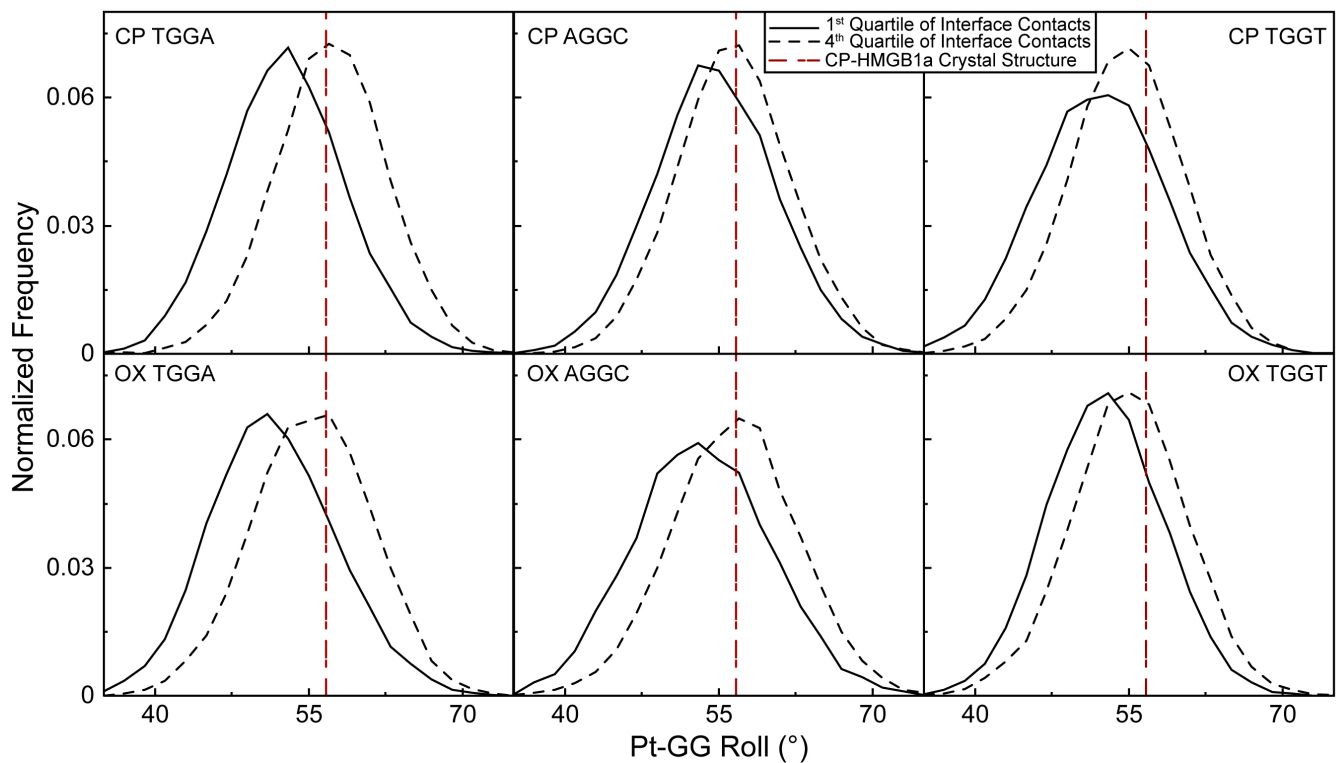


**Figure S9. Effect of roll on protein-DNA interface contacts.** Distribution of the Pt-GG roll for structures in the first and fourth quartiles of the distribution of protein-DNA interface contacts in different sequence contexts are plotted. The value of the roll in the CP-TGGA-HMGB1a crystal structure is indicated by a dashed vertical, red line for reference.

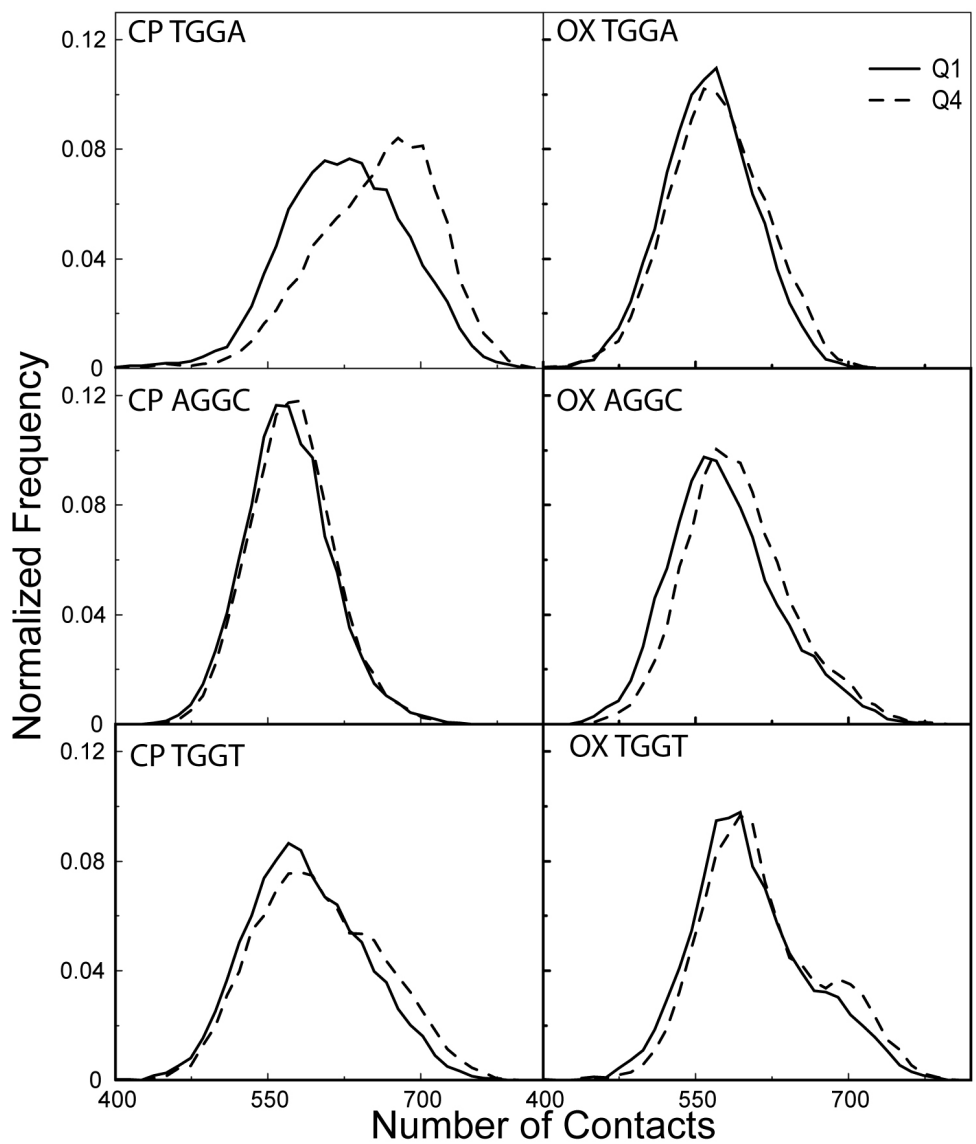


**Figure S10. Effect of Pt-GG roll on interface contacts other than Phe37 stacking.** Distribution of the number of protein-DNA interface contacts (except those formed by Phe37) of structures in the first quartile (Q1) and last quartile (Q4) of Pt-GG roll distribution in different sequence contexts.

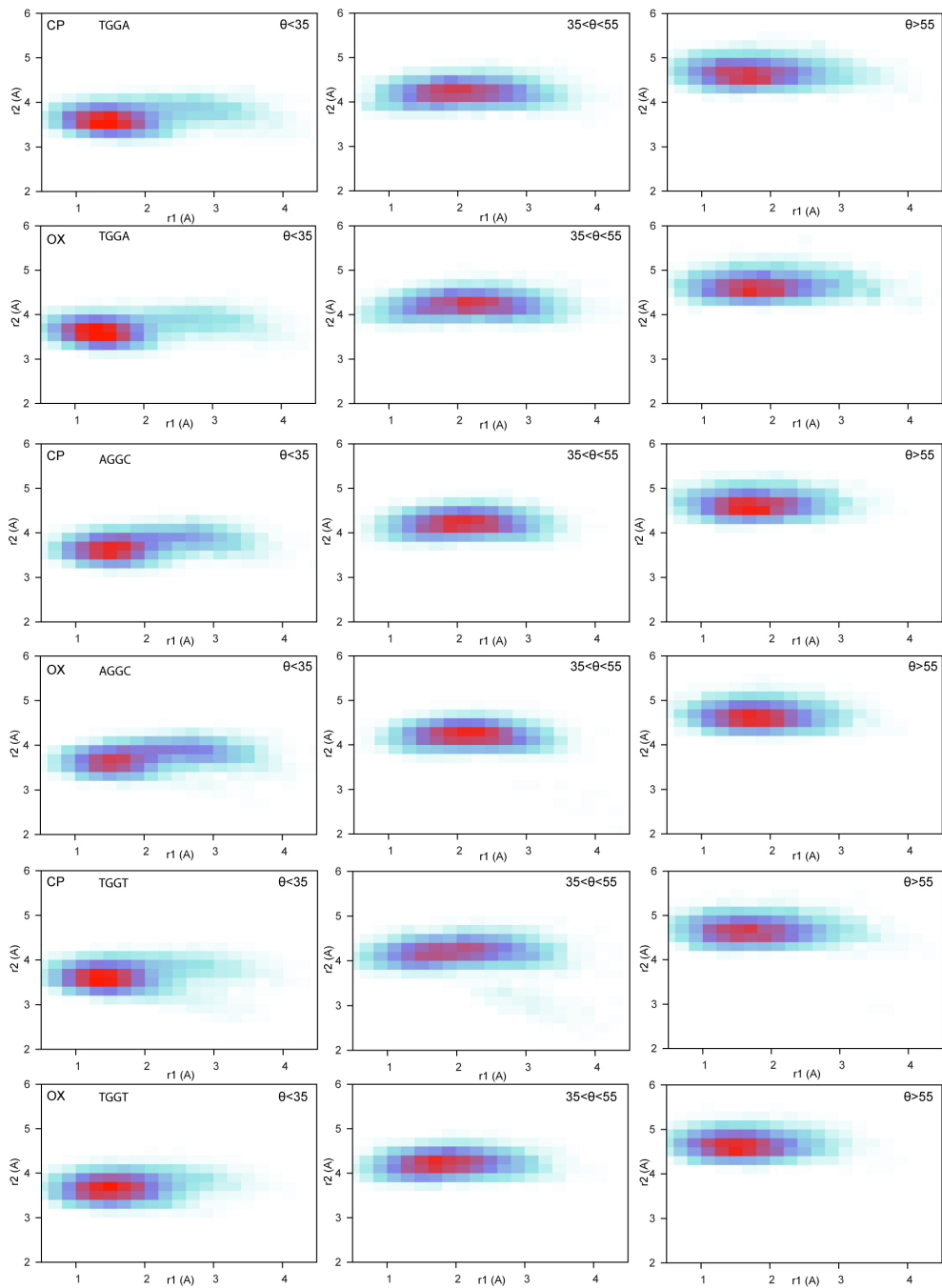


**Figure S11. Frequency of different stacking modes of Phe37 with 3' guanine.** The ensembles in different sequence contexts are divided into three groups based on the  $\theta$  value of stacking of Phe37 with 3' guanine. For each of these groups, the two dimensional histogram of  $r_1$  and  $r_2$  are plotted as a heat map. Here, higher frequency is denoted by red, lower frequency by cyan and mid-range frequency by blue.

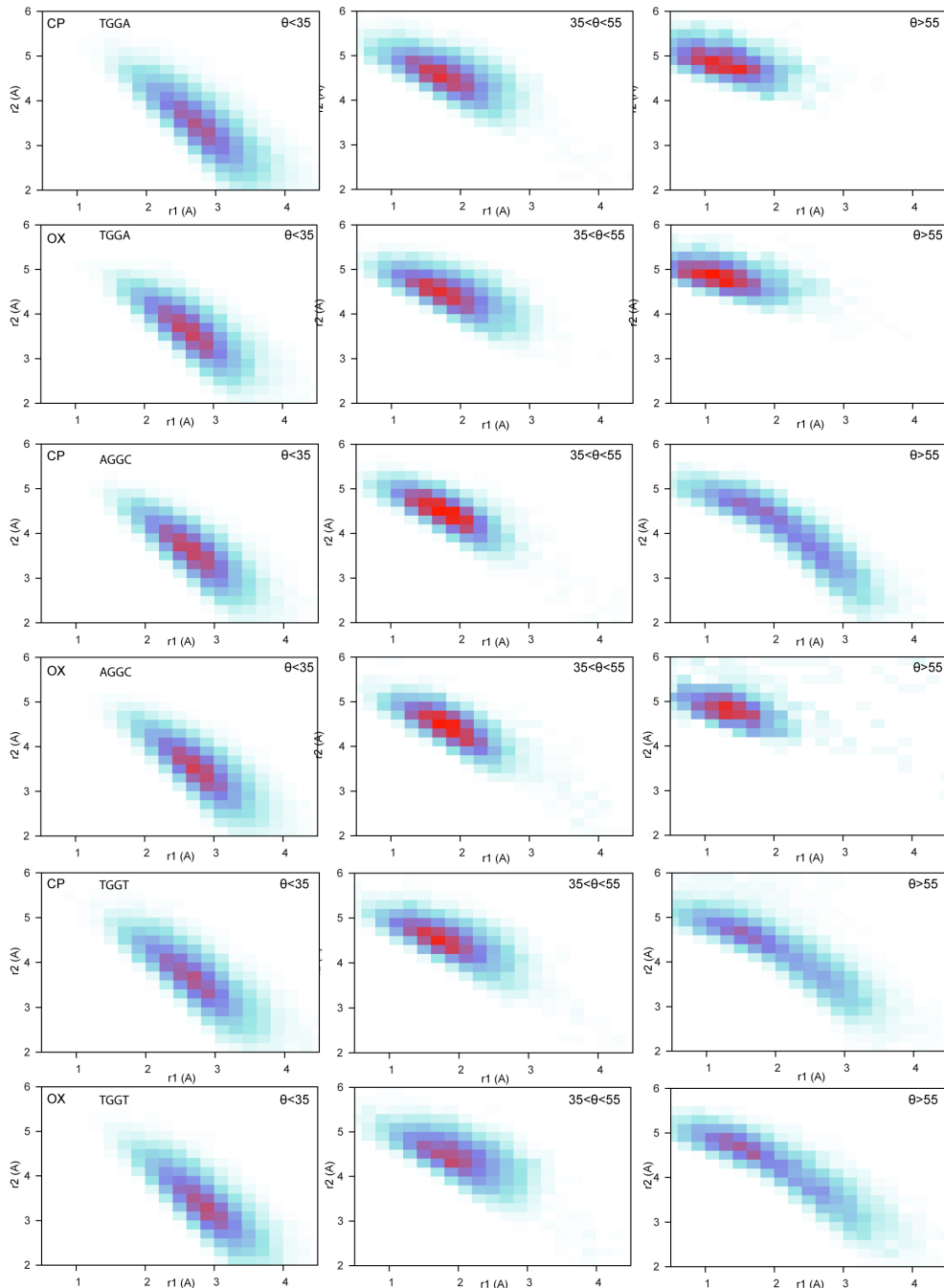


**Figure S12. Frequency of different stacking modes of Phe37 with 5' guanine.** The ensembles in different sequence contexts are divided into three groups based on the  $\theta$  value of stacking of Phe37 with 5' guanine. For each of these groups, the two dimensional histogram of  $r_1$  and  $r_2$  are plotted as a heat map. Here, higher frequency is denoted by red, lower frequency by cyan and mid-range frequency by blue.

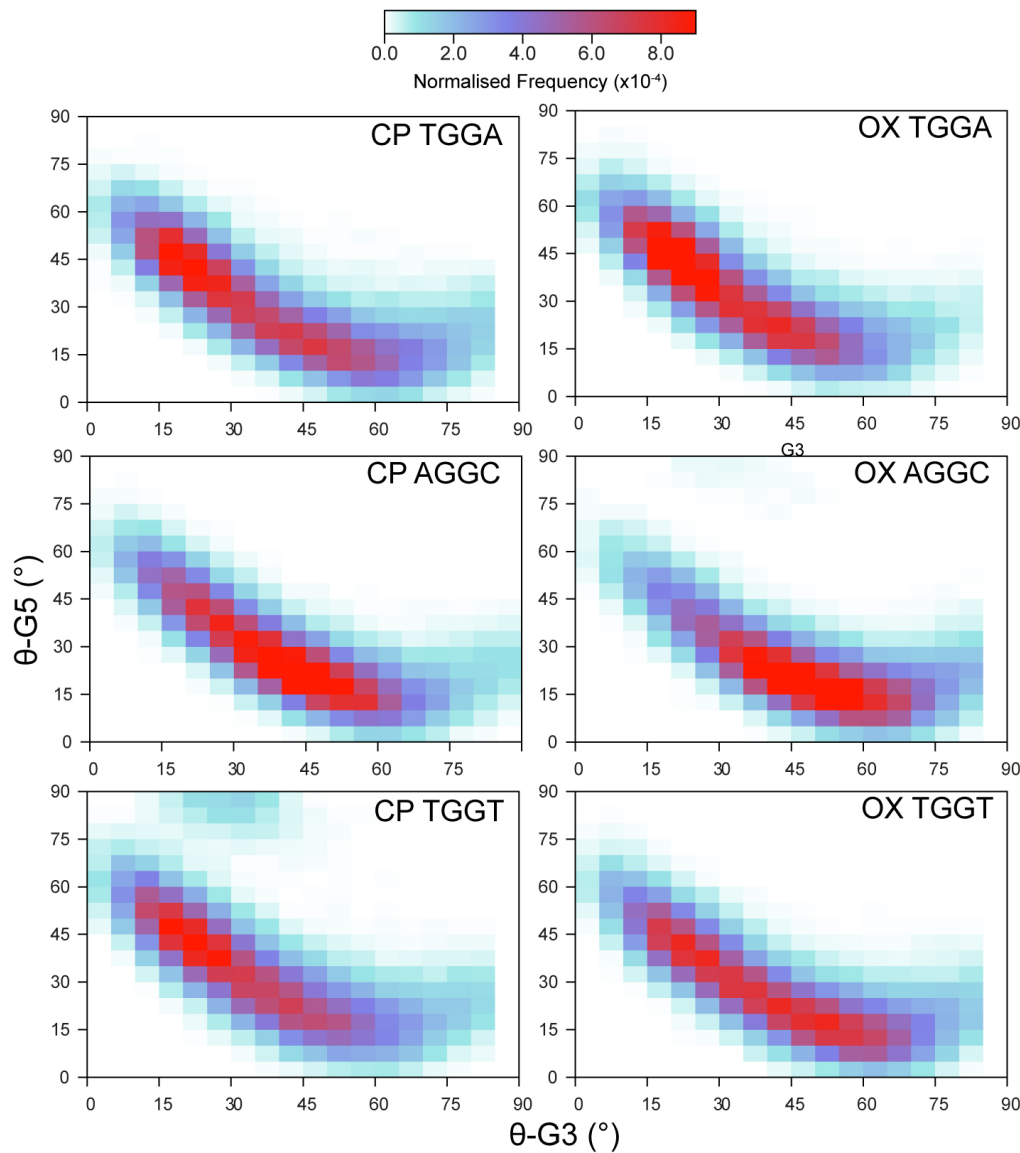


**Figure S13. Correlation of  $\theta$  values for Phe37 stacking with 3' and 5' guanine.** Two dimensional histogram of the angle between the planes of the six-membered rings of Phe37 and the 3'/5' guanine is plotted as a heat map with higher frequencies colored red and lower frequencies colored cyan.

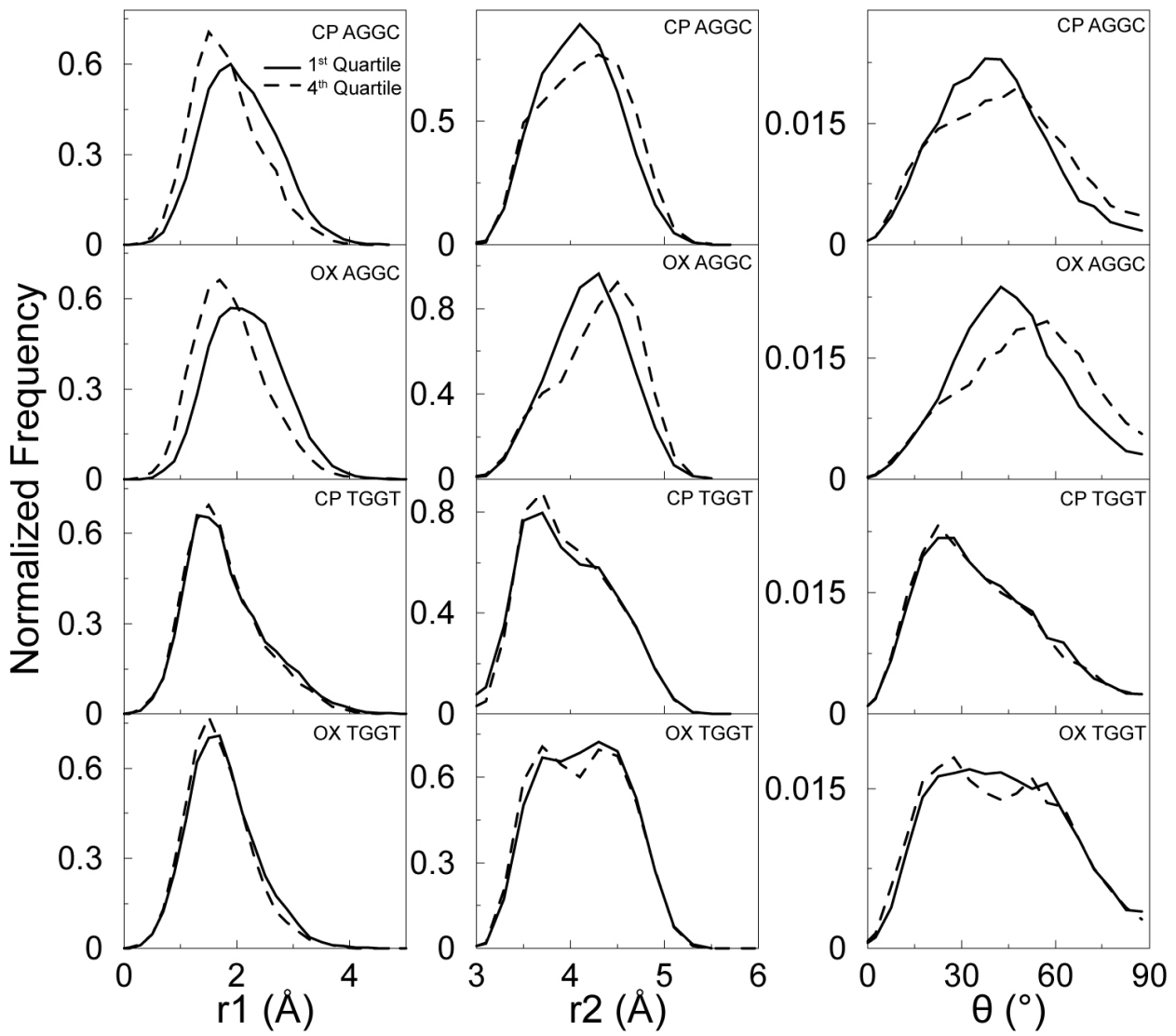


**Figure S14.** The distribution of parameters used to describe stacking of Phe37 with 3' G of the platinated base-pair ( $r_1$ ,  $r_2$  and  $\theta$ ) of CP- and OX-DNA in the AGGC and TGGT sequence contexts are plotted for the structures belonging to the first and fourth quartile of the Pt-GG roll distribution.